ELSEVIER

Journal of Alloys and Compounds 461 (2008) 160–165

Journal of ALLOYS AND COMPOUNDS

www.elsevier.com/locate/jallcom

Microstructure and adhesion strength of Sn–9Zn–1.5Ag–*x*Bi (*x* = 0 wt% and 2 wt%)/Cu after electrochemical polarization in a 3.5 wt% NaCl solution

Wang-Long Li [a,b], Ying-Ru Chen [a], Kuo-Ming Chang [a], Chih-Yao Liu [c], Min-Hsiung Hon [c], Moo-Chin Wang [d,*]

[a] *Department of Mechanical Engineering, National Kaohsiung University of Applied Sciences, 415 Chien-Kung Road, Kaohsiung 80782, Taiwan, ROC*
[b] *Institute of Nanotechnology and Microsystems Engineering, National Cheng Kung University, 1 Ta-Hsueh Road, Tainan 70101, Taiwan, ROC*
[c] *Department of Materials Science and Engineering, National Cheng Kung University, 1 Ta-Hsueh Road, Tainan 70101, Taiwan, ROC*
[d] *Faculty of Fragrance and Cosmetics, Kaohsiung Medical University, 100 Shihchuan 1st Road, Kaohsiung 80728, Taiwan, ROC*

Received 15 June 2007; received in revised form 8 July 2007; accepted 9 July 2007
Available online 19 July 2007

Abstract

The microstructure and adhesion strength of the Sn–9Zn–1.5Ag–*x*Bi (*x* = 0 wt% and 2 wt%)/Cu interface after electrochemical polarization have been studied by X-ray diffraction (XRD), scanning electron microscopy (SEM) and pull-off testing. The equilibrium potentials of Sn–9Zn–1.5Ag/Cu and Sn–9Zn–1.5Ag–2Bi/Cu are −1.31 V_{sce} and −1.22 V_{sce}, respectively, indicating that Sn–9Zn–1.5Ag–2Bi/Cu has a better corrosion resistance than that of Sn–9Zn–1.5Ag/Cu. The intermetallic compounds of Cu_6Sn_5, Cu_5Zn_8 and Ag_3Sn are formed at the soldered interface between the Sn–9Zn–1.5Ag–*x*Bi solder alloy and the Cu substrate. The scallop-shaped Cu_6Sn_5 is close to the Cu substrate and the scallop-shaped Cu_5Zn_8 is found at the interface in the solder matrix after soldering at 250 °C for 10 s. The corrosion products are $ZnCl_2$, $SnCl_2$ and ZnO. On the other hand, pits are also formed on the surface of both solder alloys. The interfacial adhesion strength of the Sn–9Zn–1.5Ag/Cu and Sn–9Zn–1.5Ag–2Bi/Cu decreases from 8.27 ± 0.56 MPa and 12.67 ± 0.45 MPa to 4.78 ± 0.45 MPa and 8.14 ± 0.38 MPa, respectively, after electrochemical polarization in a 3.5 wt% NaCl solution. The fracture path of the Sn–9Zn–1.5Ag–2Bi/Cu is along the solder alloy/ZnO and solder/Cu_6Sn_5 interfaces.

Keywords: Microstructure; Adhesion strength; Electrochemical polarization; Corrosion

1. Introduction

For electronic parts and devices, solder joints provide electrical conductivity and suitable mechanical strength [1]. Although a lot of solder alloys can be chosen, a 63Sn–37Pb eutectic solder alloy has been widely used for microsoldering in electronic assembles because of its excellent wettability and other necessary properties such as appropriate melting temperature and surface tension. However, its application in the electronic packaging industry is restrained because of its toxicity and a ground-water pollution problem, resulting in an emergent need for research on lead-free solders used in electronic industry to substitute the Pb–Sn system [2].

In order to design a new lead-free solder alloy, several important factors such as melting point, wettability, solder joint reliability, and corrosion resistance have to be considered [3,4]. A lower melting point decreases the probability for the flux of polymer matrix during the reflowing process. An excellent wettability makes Cu substrates to react with solder alloys to form intermetallic compounds (IMCs) at the interface between them. Sn–9Zn solder alloy is a promising material to be used in lead-free packaging process because its melting point of 198 °C is close to that of the 63Sn–37Pb solder alloy. Moreover, the Sn–9Zn solder alloy also has excellent mechanical properties [5]; however, it is susceptible to oxidation and corrosion.

Takemoto et al. [6] have pointed out that adding Ag to the Sn–9Zn lead-free solder alloy inhibits the anodic dissolution of Zn and enhances the wettability of the solder alloy on the Cu substrate. Chang et al. [7] have reported that the solidus temperature of the Sn–9Zn–*x*Ag solder alloy is around 197 °C, but

* Corresponding author. Tel.: +886 6 2585663; fax: +886 6 2502734.
E-mail address: mcwang@kmu.edu.tw (M.-C. Wang).

0925-8388/$ – see front matter © 2007 Elsevier B.V. All rights reserved.
doi:10.1016/j.jallcom.2007.07.026

the liquidus temperature decreases from 225.3 °C to 221.7 °C and 223.6 °C for Ag content in the solder alloy increasing from 1.5 wt% to 2.5 wt% and 3.5 wt%, respectively. Moreover, Kirkendall voids have not been found at the interface between the Sn–9Zn–*x*Ag solder alloy and the Cu substrate as reported by Chang et al. [8].

Furthermore, Chang et al. [9] have demonstrated that the Sn–9Zn–0.5Ag–1In solder alloy has a near-eutectic composition and melts at 187.6 °C with the heat fusion of 73.1 J/g. The metals of 89 wt% Sn, 9.0 wt% Zn, 1.5 wt% Ag and the addition of 0.5 wt% Bi were melted at 600 °C in a stainless steel crucible and cooled in air to form the Sn–9Zn–1.5Ag–0.5Bi near-eutectic solder alloy with the melting point and range of 195.9 °C and 10 °C, respectively, as demonstrated by Liu et al. [10]. On the other hand, the electrochemical behavior of the Sn–9Zn–*x*Ag lead-free solders in a 3.5 wt% NaCl solution have been reported by Chang et al. [11]. However, the microstructure and adhesion strength of the Sn–9Zn–1.5Ag–2Bi/Cu after polarization a 3.5 wt% NaCl solution have not yet been discussed in detail.

The microstructure and adhesion strength of the Sn–9Zn–1.5Ag–2Bi/Cu have been studied by electrochemical polarization, X-ray diffraction (XRD), scanning electron microscopy (SEM) and pull-off testing. The objective of this study are to: (i) compare the corrosion resistance of the Sn–9Zn–1.5Ag and Sn–9Zn–1.5Ag–2Bi solder alloys, (ii) identify the corrosion products for the Sn–9Zn–1.5Ag–2Bi solder alloy and (iii) determine the adhesion strength of the Sn–9Zn–1.5Ag–2Bi/Cu after polarization in a 3.5 wt% NaCl solution test.

2. Experimental procedure

The Sn–9Zn–1.5Ag–*x*Bi (*x* = 0 wt% and 2 wt%) solder alloys used in this study were melted with pure metals (purity is 99.9%) of 89. 5 wt% Sn, 9.0 wt% Zn, 1.5 wt% Ag for Sn–9Zn–1.5Ag and 87.5 wt% Sn, 9.0 wt% Zn, 1.5 wt% Ag, 2.0 wt% Bi for Sn–9Zn–1.5Ag–2Bi, respectively. They were degreased and deoxidized with 5 vol% HCl and 5 wt% NaOH solutions, respectively, rinsed with deionized water and then melted at 600 °C in a stainless steel crucible.

The substrate was an oxygen-free, high conductivity (OFHC) Cu plate and cleaned by the same procedure as mentioned above for pure metals. After cleaning, the Cu substrate was fluxed in a 3.5 wt% DMAHCl solution (3.5 wt% dimethylammonium chloride and ethanol as a solvent) for 10 s, hot-dipped in the molten solder alloy at 250 °C for 10 s and then cooled in air.

The electrochemical polarization was conducted according to the Japanese International Standard (JIS G 0597). A potentiostat (model 273, EG&G, USA) with a software was utilized to determine the over-potential of the solder alloy, a schematic diagram of the electrochemical instrument is shown in Fig. 1 [12]. A 3.5 wt% NaCl solution (Wako Pure Chemical Industries Ltd., 99.5% purity, Osaka, Japan) was used as a test medium and deacrated by N_2 with purity of 99.9% for 30 min before polarization. The sample was then connected to the cell as shown in Fig. 1, in which a Pt-coated Ti net was used as a counter electrode and the reference electrode was a saturated calomel electrode (SCE) with a stable potential of 0.244 V in a saturated KCl solution. The sample was cathodically polarized at −1.5 V_{sce} for 10 min and then from −1.7 V_{sce} to 0.5 V_{sce} at a sweeping rate of 1 mV/s. Before it, the sample was ground with sandpapers to expose the fresh surface. After it, the corrosion products on the sample surface were cleaned with acetone and determined by X-ray diffraction (XRD, D-MAX IIIβ, Rigaku, Tokyo) at a scanning rate of 2°/min for 2θ from 20° to 80°. The microstructure was observed with a scanning electron microscope (SEM, JXA-840, JEOL, Tokyo).

After the electrochemical polarization, the corrosion products on the sample surface were removed with sandpapers and the clean sample was attached to an Al stud with diameter of 0.27 cm (0.106 in.). The strength of an epoxy on an Al stud was 70 MPa. A pull-off testing was described elsewhere [10]. The instrument exerted a force on the stud at a rate of 89.0 N/s until the Al stud was separated from the sample. The adhesion strength of the Sn–9Zn–1.5Ag–2Bi/Cu interface was recorded with a computer. A total of 20 samples were measured in this study.

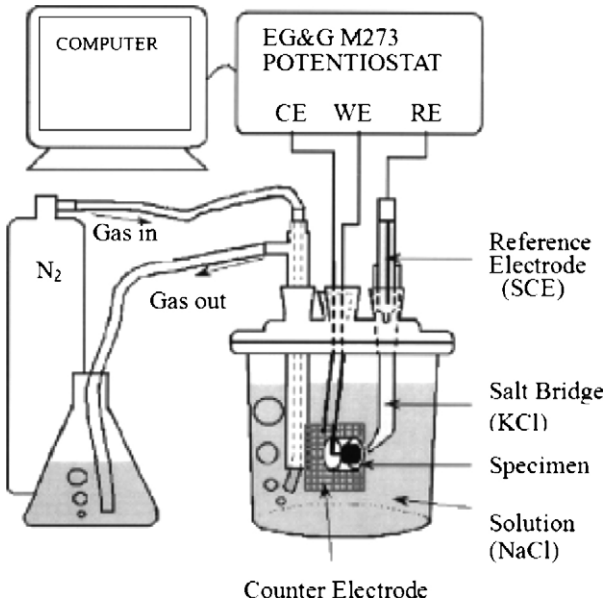

Fig. 1. Schematic diagram of electrochemical instrument.

3. Results and discussion

3.1. Phase identification of the IMCs at the Sn–9Zn–1.5Ag–xBi/Cu interface before and after the electrochemical polarization

Fig. 2 illustrates the polarization curves of the Sn–9Zn–1.5Ag–*x*Bi solder alloys with the Cu substrate in a 3.5 wt% NaCl solution. The equilibrium potentials (E_{eq}) of the Sn–9Zn–1.5Ag/Cu and Sn–9Zn–1.5Ag–2Bi/Cu are −1.31 V_{sce} and −1.22 V_{sce},

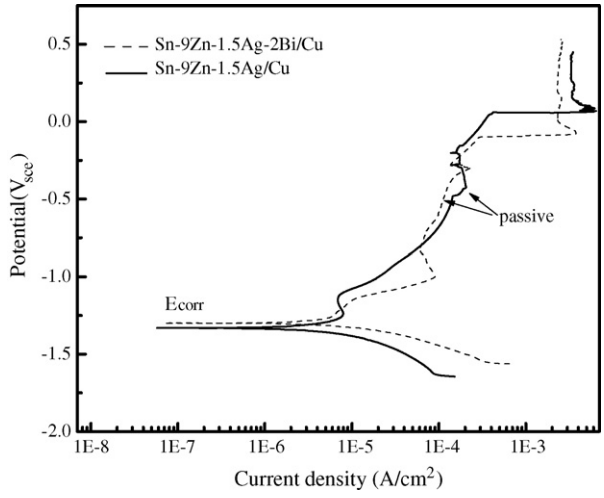

Fig. 2. Polarization curves of Sn–9Zn–1.5Ag–*x*Bi (*x* = 0 wt% and 2 wt%)/Cu in a 3.5 wt% NaCl solution.

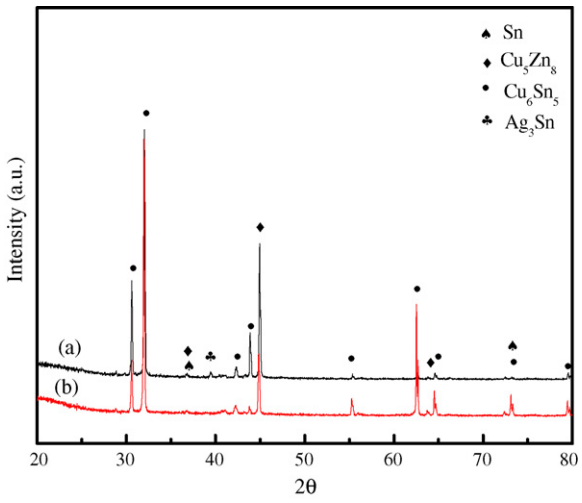

Fig. 3. XRD patterns of Sn–9Zn–1.5Ag–*x*Bi/Cu interfaces soldered at 250 °C for 10 s: (a) $x = 0$ and (b) $x = 2$.

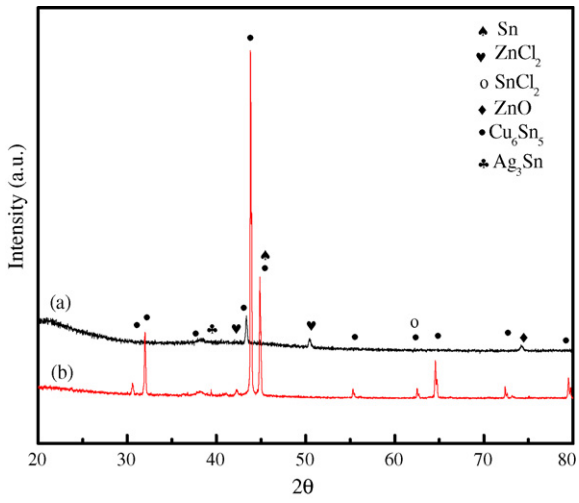

Fig. 4. XRD patterns of Sn–9Zn–1.5Ag–*x*Bi/Cu interfaces after electrochemical polarization in a 3.5 wt% NaCl solution: (a) $x = 0$ and (b) $x = 2$.

respectively, indicating that the Sn–9Zn–1.5Ag–2Bi/Cu has a better corrosion resistance than that of the Sn–9Zn–1.5Ag/Cu in a 3.5 wt% NaCl solution. Moreover, the passivation potential (E_{pass}) of the Sn–9Zn–1.5Ag/Cu is 0.15 V and the current density varies is from 10^{-4} A/cm^2 to 10^{-2} A/cm^2. When the current density also varies from 10^{-4} A/cm^2 to 10^{-2} A/cm^2, the passivation potential of the Sn–9Zn–1.5Ag–2Bi/Cu is −0.15 V. This result shows that the addition of Bi enhances the corrosion resistance.

Fig. 3 shows the XRD patterns of the Cu substrate hot-dipped in the melted Sn–9Zn–1.5Ag–*x*Bi solder alloy at 250 °C for 10 s. It indicates that Cu_6Sn_5, Cu_5Zn_8 and Ag_3Sn are formed at the interface between the Sn–9Zn–1.5Ag–*x*Bi solder alloy and the Cu substrate. This result is consistent with that of Chang et al. [13].

Yu et al. [14] have pointed out that the bcc γ-Cu_5Zn_8 layer is one of the IMC layers formed at the Sn–9Zn/Cu and Sn–Zn–Al/Cu interfaces. Ag_3Sn is formed at the solder alloy/Cu interface when the Ag content of the solder alloy is above 0.1 wt% because the solubility of Ag in Sn is quite low even at the eutectic temperature [15]. Chang et al. [16] found that Ag_3Sn is formed at the Cu/Cu_5Zn_8 interface in the Sn–9Zn–0.5Ag solder alloy. In the present study, Ag_3Sn formed at the Cu/Cu_5Zn_8 interface in the Sn–9Zn–0.5Ag solder alloy. Moreover, Ag_3Sn is observed in the XRD patterns, showing that a higher dipping temperature is beneficial to the formation of Ag_3Sn. Furthermore, the same phases appear in micrographs in Fig. 3(a) and (b), showing that the IMCs are not changed at the solder alloy/Cu interface when 2 wt% Bi is added to the Sn–9Zn–1.5Ag solder alloy system.

The XRD patterns of the Sn–9Zn–1.5Ag–*x*Bi/Cu after electrochemical polarization in a 3.5 wt% NaCl solution are shown in Fig. 4. It indicates that Ag_3Sn and Cu_6Sn_5 IMCs are retained and the corrosion products are $SnCl_2$, $ZnCl_2$ and ZnO. This result is due to that Ag_3Sn and Cu_6Sn_5 are more noble than the Sn matrix in that does not dissolve but acts as a cathode in the test [11]. Moreover, the Sn matrix acts as an anode in the electrochemical polarization, which reacts with Cl^- to form $SnCl_2$. Vincent and Richards [17] have pointed out that $ZnCl_2$ is formed in the Sn–9Zn solder alloy during the corrosion process. On the other hand, in the Zn^{2+}/H_2O system, ZnO is the most stable product [18].

3.2. *Microstructure of the Sn–9Zn–1.5Ag–xBi/Cu interface before and after the electrochemical polarization*

Fig. 5(a) illustrates the microstructure of the Sn–9Zn–1.5Ag/Cu before the electrochemical polarization. It is found that the scallop-shaped Cu_6Sn_5 is close to the Cu substrate. The scallop-shaped Cu_5Zn_8 is found at the interface in the solder matrix after soldering at 250 °C for 10 s. The Cu_5Zn_8 layer is the most stable phase at the Sn–9Zn/Cu interface as shown by the thermodynamic calculation and it is in agreement with Lee et al. [19]. For the Cu substrate dipped in the Sn–9Zn solder alloy at 350 °C for 30 s, the IMC layer is Cu_5Zn_8 as demonstrated by Chang et al. [13]. In the present study, Cu_6Sn_5 is found at the interface close to the Cu substrate and Cu_5Zn_8 is also found in the solder matrix. This result is due to the Cu diffused to the Sn–9Zn–1.5Ag solder alloy during soldering because Ag increases the solubility of Cu in Sn as demonstrated by Chada et al. [20] Because the Ag diffuses and reacts with Sn to form Ag_3Sn, on the other hand, Cu also diffuses through channels and reacts with Sn to form Cu_6Sn_5 during soldering. The more Ag addition induces the more channels for Cu diffusing and increasing the solubility in Sn. Chang et al. [21] have pointed out that the Sn–9Zn–3.5Ag/Cu interface after soldering at 350 °C for 10 s, the scallop-shaped Cu_5Zn_8 layer is found at the interface, and subsequently the scallop-shaped Cu_6Sn_5 layer has replaced the Cu_5Zn_8 at the interface close to the solder alloy after soldering for 20 s. In the present study, the IMCs are different from the result of Chang et al. [21]. This is basing on the different dipping temperature 250 °C and 350 °C for Sn–9Zn–1.5Ag and Sn–9Zn–3.5Ag solder alloy, respectively, to affect the IMCs formation.

This result is perhaps due to that the 1.5 wt% Ag addition and soldering at 250 °C make Cu diffuse to the Sn–9Zn–1.5Ag sol-

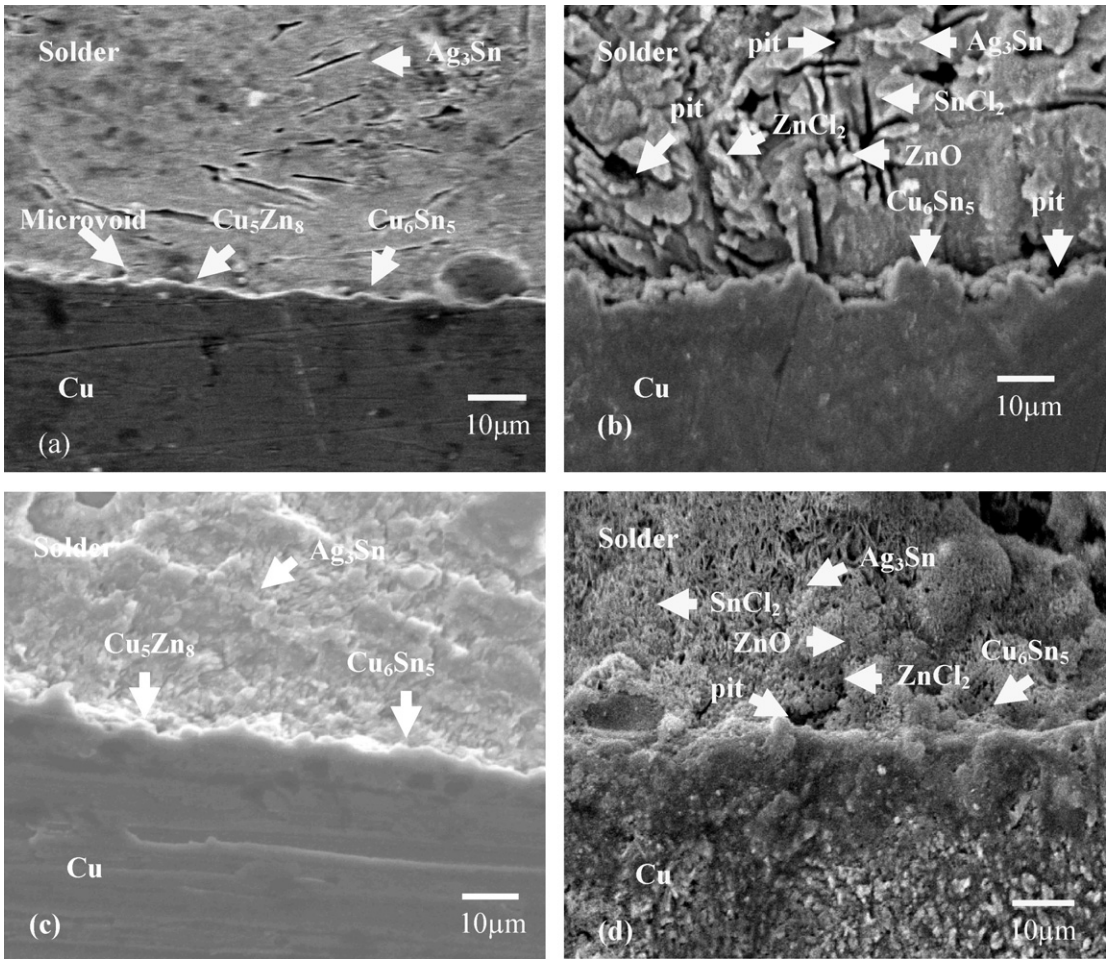

Fig. 5. SEM micrographs of Sn–9Zn–1.5Ag–*x*Bi/Cu interface: (a) as-soldered for $x = 0$, (b) after electrochemical polarization for $x = 0$, (c) as-soldered for $x = 2$ wt% and (d) after electrochemical polarization for $x = 2$ wt%.

der alloy and decrease the Cu solubility in Sn so that Cu reacts with Sn to form Cu_6Sn_5 at interface near the Cu substrate. On the other hand, Cu with Zn to form Cu_5Zn_8 in the solder matrix also creates the Cu solubility decreased. Moreover, Cu diffusion also induces the formation of microvoids at the interface. This phenomenon is caused by the solubility of Cu in Sn and Zn decreased during solidification and the precipitates in solder matrix reacted with Sn and Zn to form the Cu_6Sn_5 and Cu_5Zn_8, respectively. Therefore, not only the high diffusivity of Cu caused IMCs formation in the solder matrix, but also induced the microvoids at the interface. This result agrees with that of Chang et al. [21].

The corroded surface of the Sn–9Zn–1.5Ag/Cu interface is illustrated in Fig. 5(b), revealing that the corrosion products of $ZnCl_2$, $SnCl_2$ and ZnO and pits are found in that alloy. Chang et al. [11] have demonstrated that the formation of pits is due to the dissolution of $AgZn_3$ and Ag_5Zn_8 of the Sn–9Zn–1.5Ag solder alloy in the electrochemical polarization. But in the present study, $AgZn_3$ and Ag_5Zn_8 are not formed at the Sn–9Zn–1.5Ag/Cu interface; therefore, the pits formation may be due to the dissolution of Cu_5Zn_8. The Sn–9Zn solder alloy is reported to be sensitive to pitting corrosion [11]. On the other hand, the corrosion products of $ZnCl_2$, $SnCl_2$ and oxygen are found. Oxygen comes from the electrolysis of H_2O and is trapped in the pits to react with Zn^{2+}, forming ZnO. $ZnCl_2$ and $SnCl_2$ are formed through the adsorption of aggressive Cl^- ions at the surface of solder alloy in the protective film and their accumulation in these imperfections are considered as an important factor initiating corrosion products [22].

The microstructure of the Sn–9Zn–1.5Ag–2Bi/Cu interface soldered at 250 °C for 10 s is shown in Fig. 5(c). It indicates that the scallop-shaped of Cu_6Sn_5 and Cu_5Zn_8 are formed at the interface close to the Cu substrate. The Ag_3Sn particles are still embedded in the solder. The micrographs shown in Fig. 5(a) and (c) are the same IMCs at the interface, namely, Bi addition to the Sn–9Zn–1.5Ag solder alloy does not affect IMCs formation. The micrograph shown in Fig. 5(d) is the corrosion surface of the Sn–9Zn–1.5Ag–2Bi/Cu interface after the electrochemical polarization in a 3.5 wt% NaCl solution. It exhibits that small pits are formed in the Sn–9Zn–1.5Ag–2Bi solder alloy and the corrosion products of ZnO, $ZnCl_2$ and $SnCl_2$ are also found, agreeing with the XRD result shown in Fig. 4. On the other hand, the micrographs shown in Fig. 5(b) and (d) are the same corrosion products for the Sn–9Zn–1.5Ag and Sn–9Zn–1.5Ag–2Bi solder alloys after the electrochemical polarization, however, the pits of the Sn–9Zn–1.5Ag–2Bi solder alloy is less than that of the Sn–9Zn–1.5Ag, showing that the corrosion resistance of

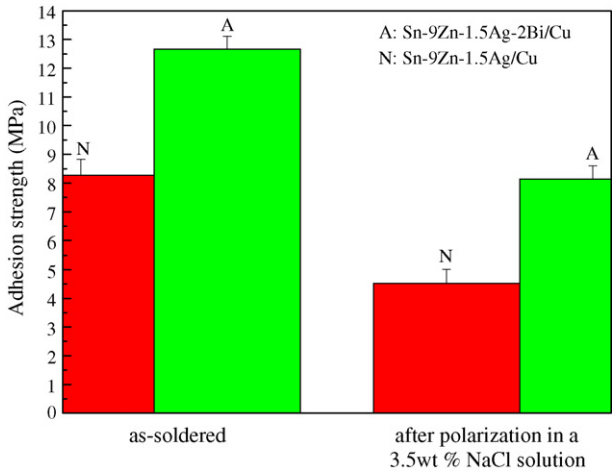

Fig. 6. Interfacial adhesion strength of Sn–9Zn–1.5Ag–*x*Bi/Cu for as-soldered and after electrochemical polarization.

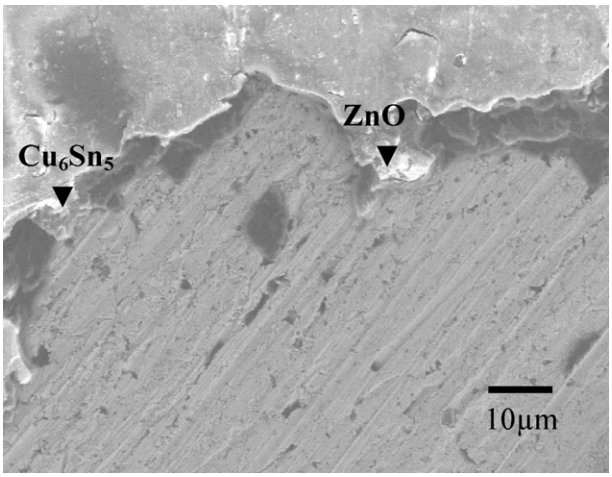

Fig. 7. Fracture micrograph of Sn–9Zn–1.5Ag–2Bi/Cu interface after electrochemical polarization.

the Sn–9Zn–1.5Ag–2Bi solder alloy is higher than that of the Sn–9Zn–1.5Ag. This result also matches the polarization curves of the Sn–9Zn–1.5Ag/Cu interface shown in Fig. 2.

3.3. Interfacial adhesion strength and fracture path of the Sn–9Zn–1.5Ag–xBi/Cu

The interfacial adhesion strength of the Sn–9Zn–1.5Ag–*x*Bi lead-free solder alloy which has been soldered on the Cu substrate at 250 °C for 10 s and electrochemically polarized in a 3.5 wt% NaCl solution is shown in Fig. 6. The adhesion strengths are 8.27 ± 0.56 MPa and 12.67 ± 0.45 MPa for the as-soldered Sn–9Zn–1.5Ag and Sn–9Zn1.5Ag–2Bi solder alloys, respectively. Bi Addition to the Sn–9Zn–1.5Ag solder alloy is beneficial to the enhancement of the adhesion strength. Liu et al. [23] have pointed out that the adhesion strength of the Sn–9Zn–1.5Ag–0.5Bi soldered on the Cu substrate at 250 °C for 60 is 12.44 ± 0.58 MPa. In the present study, although added with 1.5 wt% Bi, adhesion strength is only 12.67 ± 0.45 MPa. This is due to short soldering time, only 10 s, and the Ag_3Sn formed with the adhesion strength near 12.44 ± 0.58 MPa. Since a longer soldering time promotes the diffusion of elements and offers a higher bonding strength in the interface. On the other hand, when Cu substrate dipping in Sn–9Zn–1.5Ag–0.5Bi solder alloy at 250 °C for 60 s, the Ag_3Sn was not formed at the solder alloy/Cu interface. During aging at 150 °C for 100 h, the Ag_3Sn formed and created the adhesion strength of Sn–9Zn–1.5Ag–0.5Bi/Cu decreased from 12.44 ± 0.58 MPa to 8.57 ± 0.43 MPa [23]. This is due to IMCs growth during 150 °C aging for 100 h inducing thermal stress at IMCs layer/interdiffusion zone interface and creating the adhesion strength decreased. In addition, microvoids caused the stress concentration also reduces the adhesion strength during 150 °C aging for 100 h. [23] Moreover, the results of Fig. 6 also shown the interfacial adhesion strengths of the Sn–9Zn–1.5Ag/Cu and Sn–9Zn–1.5Ag–2Bi/Cu after the electrochemical test in a 3.5 wt% NaCl solution are 4.78 ± 0.45 MPa and 8.14 ± 0.38 MPa. The reductions in adhesion strength are 42% and 35 % for the Sn–9Zn–1.5Ag and Sn–9Zn–1.5Ag–2Bi solder alloys, respectively. This is due to the pits and corrosion products formation reduced the adhesion strength on the solder alloy/Cu interface during corrosion process in a 3.5 wt% NaCl solution. According to micrographs shown in Fig. 5(b) and (d), the pit size at the Sn–9Zn–1.5Ag–2Bi/Cu interface is smaller than at the Sn–9Zn–1.5Ag/Cu interface, agreeing with the result of Fig. 6. Moreover, the results of Figs. 2, 5 and 6 are shown that the Sn–9Zn–1.5Ag–2Bi solder alloy has a higher electrochemical resistance than the Sn–9Zn–1.5Ag alloy.

The micrograph shown in Fig. 7 is the fracture morphology of the Cu substrate dipped in the Sn–9Zn–1.5Ag–2Bi solder alloy at 250 °C for 10 s electrochemically tested in a 3.5 wt% NaCl solution. The fracture paths are along the solder alloy/ZnO and solder alloy/Cu_6Sn_5 interfaces. Yu et al. [24] have demonstrated that the fracture path of the Sn–Zn–Al solder alloy is along the Cu_5Zn_8/solder interface. Furthermore, the fracture path is along the Cu_6Sn_5/Cu_5Zn_8 interface for the Cu substrate dipped in the Sn–9Zn–1.5Ag solder alloy at 250 °C for 10 s as reported by Chang et al. [25]. The fracture paths observed in the present study is not similar to those of Yu et al. [24] and Chang et al. [25], due to ZnO are found at the Sn–9Zn–1.5Ag–2Bi/Cu interface and caused the different fracture path after electrochemical polarization.

The failure located close to the interface may result from the stress concentration at/or adjacent to the interface of the solder alloy/IMC interface, which is caused by the plastic inhomogeneity between the substrate and the solder alloy [26]. Two possible reasons are (i) stress concentration and (ii) Sn-depleted zone during the soldering process. In the present study, the soldering temperature and time are 250 °C and 10 s, respectively. This soldering condition cannot create the Sn-depleted zone due to insufficient Sn diffusion. Yu et al. [14] have demonstrated that the decrease in adhesion strength for the Zn–Al/Cu interface is due to the different coefficients of thermal expansion which cause the thermal stress at the interface between the Al, Zn-rich and Sn-rich phases. In the present study, except the thermal stress formed at the solder/IMC interface, the pits formed in the

solder alloy also create the stress concentration which lowers the strength of the matrix because of plastic inhomogeneity.

4. Conclusions

The microstructure and adhesion strength of the Sn–9Zn–1.5Ag–*x*Bi/Cu interface after electrochemical polarization in a 3.5 wt% NaCl solution have been studied by XRD, SEM and pull-off testing. The Sn–9Zn–1.5Ag–2Bi/Cu of equilibrium potential is $-1.31\,V_{sce}$ rather than that of $-1.22\,V_{sce}$ for Sn–9Zn–1.5Ag/Cu. Cu_5Zn_8, Cu_6Sn_5 and Ag_3Sn IMCs are formed at the as soldered Sn–9Zn–1.5Ag–*x*Bi/Cu interface. After electrochemical polarization in a 3.5 wt% NaCl solution, the corrosion products of $SnCl_2$, $ZnCl_2$ and ZnO are formed on the surface of both solder alloys with the pits formed on the surface of both solder alloys. Due to the greater pit size caused much more stress concentration on the Sn–9Zn–1.5Ag/Cu than the Sn–9Zn–1.5Ag–2Bi/Cu, the interfacial adhesion strength is 8.14 ± 0.38 MPa for the Sn–9Zn–1.5Ag–2Bi/Cu rather than that of 4.78 ± 0.45 MPa for Sn–9Zn–1.5Ag/Cu after electrochemical polarization. The fracture paths of the Sn–9Zn–1.5Ag–2Bi/Cu are along the interface of the solder alloy/ZnO and solder alloy/Cu_6Sn_5 after electrochemical polarization in a 3.5 wt% NaCl solution. In summary, Sn–9Zn–1.5Ag–2Bi solder alloy is with a better electrochemical resistance and can be considered as one of candidates to substitute Sn–37Pb solder alloy.

Acknowledgements

This work was supported by the National Science Council of Taiwan under Contract Nos. NSC89-2216-E-151-011 and NSC95-2221-E-151-007, which is greatly acknowledged. Experimental collaboration and suggestions from Prof. M.P. Hung and Mr. H.Y. Hwang are also very much appreciated. Many thanks are also extended to National Chia-Yi Industrial High School for offering some research facilities.

References

[1] J.W. Yoon, C.B. Lee, S.B. Jung, Mater. Trans. 43 (2002) 1820–1826.
[2] I. Shohji, T. Nakamura, F. Mori, S. Fujiuchi, Mater. Trans. 43 (2002) 1420–1428.
[3] J. Glazer, Int. Mater. Rev. 40 (1995) 65–72.
[4] M. Abtew, G. Selvaduray, Mater. Sci. Eng. 27 (2000) 95–141.
[5] M. McCormack, S. Jin, H.S. Chen, J. Electron. Mater. 23 (1994) 715–720.
[6] T. Takemoto, T. Funaki, A. Matsunawa, J. Jpn. Weld. Soc. 17 (1999) 251–256.
[7] T.C. Chang, M.C. Wang, M.H. Hon, Metall. Mater. Trans. 36A (2005) 3019–3029.
[8] T.C. Chang, M.C. Wang, M.H. Hon, J. Cryst. Growth 250 (2003) 236–243.
[9] T.C. Chang, J.W. Wang, M.C. Wang, M.H. Hon, J. Alloys Compd. 422 (2006) 239–243.
[10] C.Y. Liu, M.C. Wang, M.H. Hon, J. Electron. Mater. 33 (2004) 1557–1560.
[11] T.C. Chang, M.H. Hon, M.C. Wang, D.Y. Lin, Electrochem. Soc. 151 (2004) C484–C491.
[12] T.F. Wu, T.P. Cheng, W.T. Tsai, J. Nucl. Mater. 295 (2001) 233–243.
[13] T.C. Chang, M.C. Wang, M.H. Hon, J. Cryst. Growth 252 (2003) 391–400.
[14] S.P. Yu, M.C. Wang, M.H. Hon, J. Mater. Res. 16 (2001) 76–82.
[15] S.H. Huh, K.S. Kim, K. Suganuma, Mater. Trans. 42 (2001) 739–745.
[16] T.C. Chang, M.H. Hon, M.C. Wang, Mater. Trans. 45 (2004) 606–613.
[17] J.H. Vincent, B.P. Richards, Circuit World 19 (1993) 33–43.
[18] R. Grauer, Werkst. Korros 31 (1980) 837.
[19] B.J. Lee, N.M. Hwang, H.M. Lee, Acta Mater. 45 (1997) 1867–1874.
[20] S. Chada, R.A. Fournelle, W. Laub, D. Shangguan, J. Electron. Mater. 29 (2000) 1214–1221.
[21] T.C. Chang, M.H. Hon, M.C. Wang, Electrochem. Solid State Lett. 7 (2) (2004) J4–J7.
[22] A. Aballe, M. Bethencourt, F.J. Botana, M.J. Cano, M. Marcos, Corros. Sci. 43 (2001) 1657–1674.
[23] C.Y. Liu, M.C. Wang, M.H. Hon, J. Electron. Mater. 35 (2006) 966–971.
[24] S.P. Yu, M.H. Hon, M.C. Wang, J. Electron. Mater. 29 (2000) 237–243.
[25] T.C. Chang, M.H. Hon, M.C. Wang, J. Electron. Mater. 32 (2003) 516–522.
[26] D.R. Frear, S.N. Burchett, H.S. Morgan, J.H. Lau, The Mechanics of Solder Alloy Interconnects, Van Nostrand Reinhold, New York, 1994, p. 62.